Anisotropic Diffusion of Small Penetrants in the δ Crystalline Phase of Syndiotactic Polystyrene: A Molecular Dynamics Simulation Study

Giuseppe Milano* and Gaetano Guerra

Dipartimento di Chimica, Università di Salerno, Baronissi, 84081 Salerno, Italy

Florian Müller-Plathe

Max-Planck-Institut für Polymerforschung, D-55128 Mainz, Germany

Received December 7, 2001. Revised Manuscript Received February 20, 2002

The diffusional behavior of helium and carbon dioxide in crystalline syndiotactic polystyrene, in its nanoporous δ form, has been studied by means of molecular simulation. Crystallographic directions corresponding to prevailing diffusion pathways between crystalline cavities have been determined. Moreover, diffusion coefficients and their anisotropy at different temperatures have been calculated. For both gases at all temperatures, preferential diffusion pathways are parallel to the crystallographic *ac* planes, corresponding to rows of parallel helices with minimum interchain distances. Diffusion of carbon dioxide is slower and more anisotropic than that of helium. For both gases, the preferred diffusion pathways are along the ⟨101⟩ directions at low temperatures while parallel to the chain axes at high temperatures.

Introduction

In the past decade, it has become possible to investigate sorption and diffusion of small molecules in polymeric media by means of molecular simulations.[1,2] Most attention of computational and experimental studies has been devoted to amorphous polymers. In fact, also for semicrystalline polymers, the diffusivity is largely determined by that of their amorphous phases.[3,4] This behavior is a consequence of the lower density, associated with the less efficient packing of polymer chains generally observed in the amorphous domains, which leads to more space being available to the penetrant.

In most cases, the sorption and diffusion behavior of small molecules in semicrystalline polymeric samples can be rationalized by assuming negligible contributions from the crystalline phase. For isotactic poly(4-methyl-1-pentene) (PMP), however, the density of the crystalline phase is close to that of the amorphous phase. In that case, as pointed out by Paul and co-workers[5] and studied by means of molecular dynamics (MD) simulations by Müller-Plathe,[6] penetrant solubility and diffusivity in the crystalline phase are still lower with respect to those of the amorphous phase but not negligible.

Recent studies relative to the polymorphic behavior of syndiotactic polystyrene (s-PS) have shown that one of the four crystalline forms (the δ form) is nanoporous and has a density (0.977 g cm^{-3}) definitely lower than that of amorphous s-PS (1.04 g cm^{-3}), which is close to that of atactic polystyrene.[7]

The monoclinic structure of the δ form of s-PS (space group $P2_1/a$, $a = 1.75$ nm, $b = 1.18$ nm, $c = 0.78$ nm, and $\gamma = 118°$) has per unit cell two identical cavities centered on the center of symmetry, bounded by 10 phenyl rings (Figure 1).[7,8] These cavities are large enough to absorb as guests, without any substantial distortion of the host lattice, penetrants as large as 1,2-dichloroethane.[8,9] Moreover, associated with small distortions of the lattice (essentially increases of the *b* axis up to 10−15%), bigger guests, such as toluene or naphthalene, can be hosted.[8,10] A complete filling of the cavities by guest molecules generates clathrate structures generally presenting an organization of the polymeric host very similar to that observed for the δ form. Suitable procedures for guest removal, generally involving its replacement by more volatile temporary guests (like acetone, CS_2, or CO_2), allow easy regeneration of the nanoporous form.[11]

Sorption studies from liquid and gas phases have shown that δ form s-PS samples are able to absorb

* To whom correspondence should be addressed. E-mail: milano@chem.unisa.it.

(1) Müller-Plathe, F. *Acta Polym.* **1994**, *45*, 259.
(2) Gusev, A.; Müller-Plathe, F.; van Gusteren, W. F.; Suter, U. W. *Adv. Polym. Sci.* **1994**, *116*, 207.
(3) Crank, J., Park, G. S., Eds. *Diffusion in Polymers*; Academic: London, 1968.
(4) Comyn, J., Ed. *Polymer Permeability*; Elsevier: London, 1985.
(5) Puleo, A. C.; Paul, D. R.; Wong, P. K. *Polymer* **1989**, *30*, 1357.
(6) Müller-Plathe, F. *J. Chem. Phys.* **1995**, *103*, 4346.
(7) De Rosa, C.; Guerra, G.; Petraccone, V.; Pirozzi, B. *Macromolecules* **1997**, *30*, 4147.
(8) Milano, G.; Venditto, V.; Guerra, G.; Cavallo, L.; Ciambelli, P.; Sannino, D. *Chem. Mater.* **2001**, *13*, 1506.
(9) De Rosa, C.; Rizzo, P.; Ruiz de Ballesteros, O.; Petraccone, V.; Guerra, G. *Polymer* **1999**, *40*, 2103.
(10) Chatani, Y.; Shimane, Y.; Inoue, Y.; Inagaki, T.; Ishioka, T.; Ijitsu, T.; Yukinari, T. *Polymer* **1992**, *33*, 488.
(11) (a) Guerra, G.; Manfredi, C.; Rapacciuolo, M.; Corradini, P.; Mensitieri, G.; Del Nobile, M. A. (CNR). Ital. Patent RM94A003, 1994. (b) Reverchon, E.; Guerra, G.; Venditto, V. *J. Appl. Polym. Sci.* **1999**, *74*, 2077.

10.1021/cm011297i CCC: $22.00
Published on Web 06/11/2002

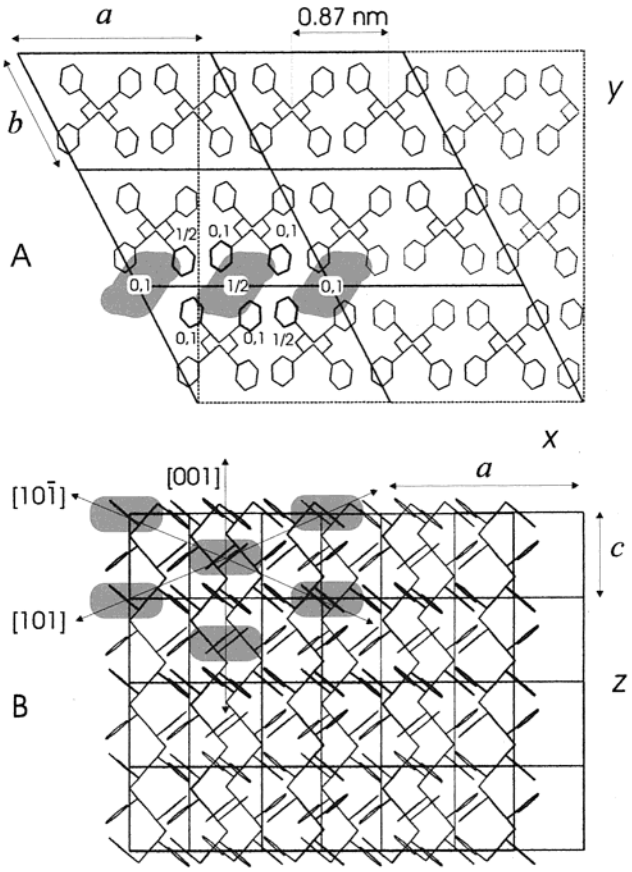

Figure 1. δ-form s-PS structure considered in our calculations. The periodic system, shown for two different views, along the *c* direction (A) and perpendicular to the *ac* plane (B), consists of four cells stacked in the *c* direction, two along the *a* direction, and three along the *b* direction. Gray regions indicate the cavities characterizing the nanoporous structure. Dashed lines show the orthorhombic box adopted in our calculations. Ten phenyl rings which bound the cavity (at height $^1/_2c$) are pointed out by darker lines in part A. The crystallographic directions connecting neighboring cavities are indicated in part B.

suitable guest molecules even when present at very low concentrations.[12−14] In particular, it has been clearly demonstrated that for sorption at low penetrant activities the penetrant is absorbed essentially only as a guest into the crystalline phase.[13,15] For this behavior, polymer materials based on this nanoporous form have been denoted as *thermoplastic molecular sieves*.[8,14]

Very recently, s-PS films in the nanoporous δ form with a high degree of orientation have been obtained.[16] They should allow an experimental characterization of the possibly anisotropic diffusion of small molecules in the δ form of s-PS.

Several aspects of s-PS-based thermoplastic materials have been studied by different molecular modeling methods: evaluation of cavity volumes,[8,17] host−guest interactions,[18] and guest conformational selectivity.[14,19] No attempt has yet been made to model the diffusion of small molecules in the nanoporous δ form.

In the present paper, we use MD simulations techniques to understand the diffusive behavior of helium and CO_2 in the crystalline δ phase of s-PS and particularly its anisotropy as a function of temperature. The diffusion of CO_2 is particularly relevant because, at present, extraction procedures by CO_2 represent the most efficient way to remove guest molecules from s-PS clathrate phases and regenerate δ form crystal phases.[11] These studies complement ongoing experimental work.[16] The main advantage of the simulations is that a well-defined and purely crystalline system can be studied, whereas the experiment has to cope with semicrystallinity (i.e., fraction of amorphous material generally larger than 0.5), incomplete orientation of the δ crystallites, and the general difficulty of measuring anisotropic diffusion coefficients.

Computational Methods

The polymer starting structure was taken from the experimental X-ray structure.[7] The unit cell of s-PS in the δ form is monoclinic with $a = 1.75$ nm, $b = 1.18$ nm, $c = 0.78$ nm, and $\gamma = 118°$. We took the *c* axis as the Cartesian *z* axis, and we considered, as shown in Figure 1, a periodic system of four cells stacked in the *c* direction, two along the *a* direction, and three along the *b* direction. To save considerable computer time, we applied orthorhombic periodic boundary conditions using a procedure developed by some of us.[20] The monoclinic *a* and *c* crystal vectors coincide with the Cartesian *x* and *z* directions of the simulation box, respectively. The *y* direction of the simulation box forms an angle θ of 27° with the *b* axis and is perpendicular to the *ac* plane. In this way, the monoclinic periodic replication properties of the unit cell could be obtained by *quasi-orthorhombic* boundary conditions (the exact angle between *x* and *y* axes would be 88°). The simulated host polymer contains 3072 atoms (cf. Figure 1).

Equilibrated structures of the pure polymer (200 ps at constant temperature and pressure) were used as starting structures for the polymer/penetrant systems. Twelve penetrant molecules were successively placed into host cavities to improve the statistical efficiency. To avoid artifacts from the accumulation of penetrants, they have been placed in nonadjacent cavities.

For the polymer, we used an all-atom force field which some of us used previously to study atactic-PS-based systems and their properties including solvent-swollen phases,[21] carbon dioxide diffusion coefficients,[22] and free-volume evaluations for simulation of positronium annihilation spectra.[23] The adopted helium force field has been applied to study different properties.[24] The

(12) Manfredi, C.; Del Nobile, M. A.; Mensitieri, G.; Guerra, G.; Rapacciuolo, M. *J. Polym. Sci., Polym. Phys. Ed.* **1997**, *35*, 133.
(13) Guerra, G.; Manfredi, C.; Musto, P.; Tavone, S. *Macromolecules* **1998**, *31*, 1329.
(14) Guerra, G.; Milano, G.; Venditto, V.; Musto, P.; De Rosa, C.; Cavallo, L. *Chem. Mater.* **2000**, *12*, 263.
(15) Musto, P.; Manzari, M. G.; Guerra, G. *Macromolecules* **1999**, *32*, 2770.
(16) Rizzo, P.; Lamberti, M.; Albunia, A.; Ruiz de Ballesteros, O.; Guerra, G., *Macromolecules*.
(17) Guerra, G.; Milano, G.; Venditto, V.; Loffredo, F.; Ruiz de Ballesteros, O.; Cavallo, L.; De Rosa, C. *Makromol. Chem., Macromol. Symp.* **1999**, *138*, 131.
(18) Milano, G.; Guerra, G.; Cavallo, L. *Eur. J. Inorg. Chem.* **1998**, *10*, 1513.
(19) Milano, G.; Guerra, G.; Cavallo, L. *Macromol. Theory Simul.* **2001**, *10*, 349.
(20) Biermann, O.; Hädicke, E.; Koltzenburg, S.; Müller-Plathe, F. *Angew. Chem., Int. Ed.* **2001**, *40*, 3822.
(21) Müller-Plathe, F. *Macromolecules* **1996**, *29*, 4782.
(22) Schmitz, H. Ph.D. Thesis, University of Mainz, Mainz, Germany, 2000.
(23) Schmitz, H.; Müller-Plathe, F. *J. Chem. Phys.* **2000**, *112*, 1040.

force field of CO_2 has been used in previous simulation studies of diffusion in PMP.[6] Details about force fields are reported in the references. An important point is the singularity-free treatment of O−C−O linear bond angle terms.[6]

MD simulations have been carried out using the YASP suite of programs.[25] MD was run at constant temperature T and constant pressure P, by weak coupling[26] to a temperature bath of the appropriate target temperature (see below) and a pressure bath of 101.3 kPa. The coupling time was 0.2 ps (T) and 0.5 ps (P) and the isothermal compressibility 10^{-6} kPa^{-1}. The time step was 2 fs. Carbon−hydrogen bond lengths were constrained using the SHAKE[27,28] algorithm. For C−C bonds of the polymer, harmonic potential energy terms (force constants of 420 000 kJ mol^{-1} nm^{-2}) were used in place of constraints. This was necessary because of the way the constraints' contribution to the pressure is calculated in YASP.[25] For nonbonded interactions, a cutoff distance of 1.0 nm was used with a reaction-field correction for the Coulombic interactions;[29] the effective dielectric constant of the continuum ϵ_{RF} was taken to be 2.5 (experimental dielectric constants of 2.3 for liquid benzene and ∼2.5 for amorphous PS). An atomic Verlet neighbor list[30] was used, which was updated every 15 time steps; neighbors were included if they were closer than 1.1 nm. Configurations were saved every 100 time steps. For both considered systems helium/polymer and CO_2/polymer, equilibrations of 200 ps followed by production runs of 4 ns have been performed.

Comparison between mean values of simulation box lengths $\langle L_x \rangle$, $\langle L_y \rangle$, and $\langle L_z \rangle$ and corresponding experimental lengths related to lattice constants shows that $\langle L_x \rangle = 3.33$ nm is smaller than that obtained from the experimental a lattice constant of $2a = 3.50$ nm. As for $\langle L_y \rangle = 3.32$ nm, its value is bigger than the one from the b lattice constant ($3b \cos \theta = 3.13$ nm). The $\langle L_z \rangle$ value of 3.11 nm is essentially equal to the experimental $4c$ value of 3.12 nm. Thus, deviations for the simulation box dimension in the xy (=ab) plane have been found. Hence, the reproduction of mean distances between neighboring polymer chains in this plane has also been checked. In particular, according to the chain packing model proposed by X-ray diffraction studies,[7] polymer chains are spaced at $a/2 = 0.87$ nm and $b = 1.185$ nm along the a and b directions, respectively. In the simulation of the empty polymer at 25 °C, we found distances of 0.83 and 1.10 nm, respectively. Deviations found for simulation box dimensions and distances between helices could be connected with orthorhombic boundary conditions. In particular, to change from monoclinic to orthorhombic boundary conditions, the value of γ was increased by 2°. In this way the unit cell volume is shrunk. During constant-pressure simulations, the system expanded to release the stress. It did this by further increasing γ. The view that this is a stress relaxation is supported by the average area of the ab plane being nearly the same as that in the experimental unit cell. From X-ray, (1.75)(1.042) = 1.823 nm^2, and from simulations of empty s-PS at 25 °C, we have (1.67)(1.107) = 1.849 nm^2; i.e., the difference is 1.3%. Because there is a minute compression in z, the resulting difference in density is less than 1%.

Results and Discussion

Diffusion Pathways. Helium atom pathways obtained from simulation trajectories at 25 and 80 °C are shown in Figure 2 for ab and ac projections of the δ crystal unit cells. Diffusion proceeds by hopping between different crystalline cavities. For some period of time, the penetrant stays in a cavity region. During such a quasi-stationary period, it explores this region but does not move beyond the cavity confines. The quasi-stationary periods are interrupted by quick leaps from one cavity into a neighboring one. Similar motion patterns have been found in all MD studies of the diffusion of small penetrants in amorphous polymers. However, because for the nanoporous δ form of s-PS all cavities are of the same size and occupy well-defined crystallographic positions, jumps between different cavities generally occur along well-defined directions. For both temperatures, the hopping between cavities generally occurs along directions which are parallel to the crystalline ac planes (Figure 2A,C). This behavior can be easily rationalized by the presence in these planes of rows of parallel helices with minimum interchain distances (0.87 nm; Figure 1A). In fact, most jumps occur along [101] and [10$\bar{1}$] directions (that is, along the family of directions ⟨101⟩) or along the c axis (or the [001] direction).

It is worth noting that the distance between two neighboring cavities is much larger along the ⟨101⟩ direction (1.9 nm) than along the [001] direction (0.78 nm = c). Nevertheless, at room temperature, jumps along ⟨101⟩ directions are favored (Figure 2B).

At higher temperature, the penetrant's pathway appears to be quite different (Figure 2C,D). The cavities are still visible, but they are explored less thoroughly because the stationary periods between leaps are shorter. Although many more leaps occur along ⟨101⟩ directions, that prevail at room temperature, most leaps occur along the chain axes, that is, along the c [001] direction (Figure 2D).

Diffusion Coefficients. The diffusion coefficient D was calculated from center-of-mass mean-square displacement curves of the penetrants[1]

$$6D = \frac{\mathrm{d}}{\mathrm{d}t} \langle |R_i(t) - R_i(0)|^2 \rangle$$

where $R_i(t)$ is the position of the ith penetrant's center of mass at time t. Averaging is performed over all penetrant molecules as well as over time origins.

Diffusion coefficients of helium and carbon dioxide for different temperatures are given in Tables 1 and 2,

(24) Maitland, G. C.; Rigby, M.; Smith, E. B.; Wakeham, W. A. *Intermolecular forces*: *their origin and determination*; Claredon Press: Oxford, U.K., 1983.
(25) Müller-Plathe, F. *Comput. Phys. Commun.* **1993**, *78*, 77.
(26) van Gunsteren, W. F.; Berendsen, H. J. C. *Angew. Chem., Int. Ed. Engl.* **1990**, *29*, 992.
(27) Ryckaert, J. P.; Ciccotti, G.; Berendsen, H. J. C. *J. Comput. Phys.* **1977**, *23*, 327.
(28) Müller-Plathe, F.; Brown, D. *Comput. Phys. Commun.* **1993**, *78*, 77.
(29) Ceperley, D., Ed. *Reaction field method for polar fluids*; NRCC Workshop Proceedings; NRCC: Ottawa, Ontario, Canada, 1980; Vol. 9, p 45.
(30) Fincham, D.; Ralston, B. J. *Comput. Phys. Commun.* **1981**, *23*, 127.

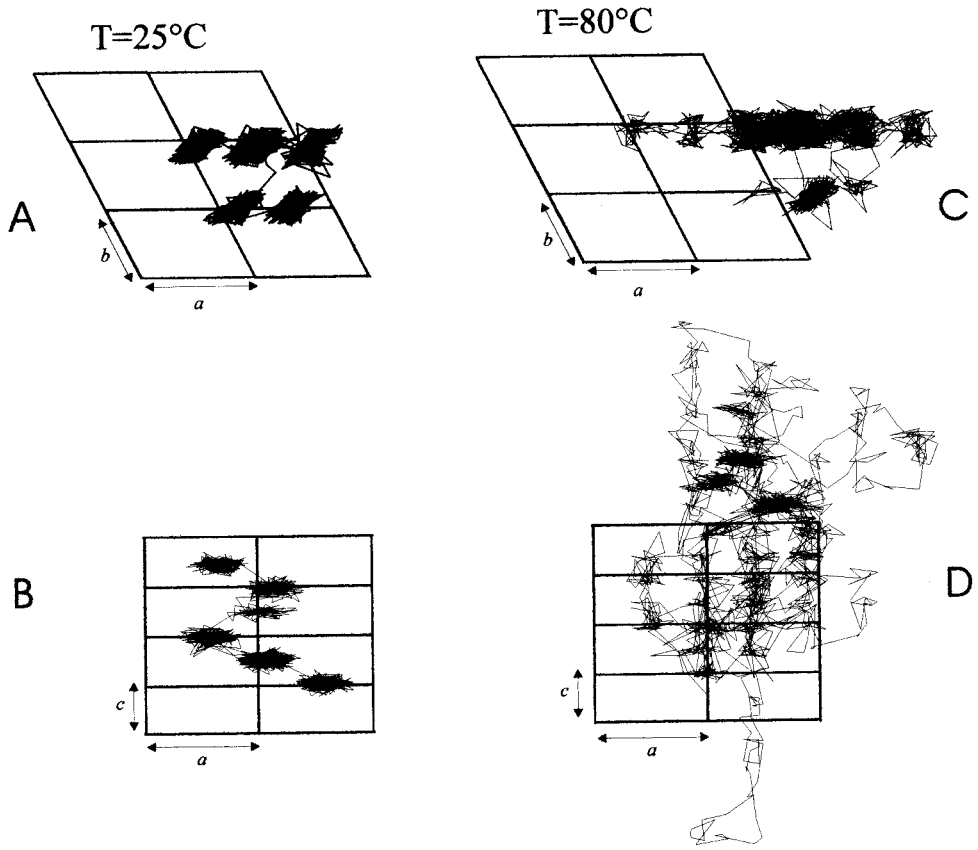

Figure 2. Trajectory (trace) of one helium atom in crystalline s-PS in its nanoporous δ form during 2 ns of simulations at (A and B) 25 °C and (C and D) 80 °C. Similarly to Figure 1, different views along the *c* direction (A and C) and perpendicular to the *ac* plane (B and D) are shown. At room temperature (A and B), a hopping motion mechanism between different crystalline cavities, prevailing along ⟨101⟩ directions, is apparent. Pathways at 80 °C (C and D) could be interpreted as penetrant motion mainly along the [001] and ⟨101⟩ directions.

Table 1. Helium Diffusion Coefficients ($cm^2\ s^{-1}$) for Different Temperatures in δ-Form s-PS

	diffusion coefficient ($cm^2\ s^{-1}$)[a]		diffusion coefficient ($cm^2\ s^{-1}$)[a]
	T = 25 °C		
D_a (=D_x)	7.9×10^{-6}	D	3.7×10^{-6}
$D_{\perp ac}$ (=D_y)	1.1×10^{-6}	$D_a/D_{\perp ac}$	7.2
D_c (=D_z)	2.0×10^{-6}	D_a/D_c	3.9
	T = 60 °C		
D_a (=D_x)	2.7×10^{-5}	D	1.2×10^{-5}
$D_{\perp ac}$ (=D_y)	1.5×10^{-6}	$D_a/D_{\perp ac}$	17
D_c (=D_z)	9.0×10^{-6}	D_a/D_c	3.0
	T = 70 °C		
D_a (=D_x)	4.3×10^{-5}	D	8.5×10^{-5}
$D_{\perp ac}$ (=D_y)	2.9×10^{-6}	$D_a/D_{\perp ac}$	15
D_c (=D_z)	2.1×10^{-4}	D_a/D_c	0.20
	T = 80 °C		
D_a (=D_x)	5.5×10^{-5}	D	8.1×10^{-5}
$D_{\perp ac}$ (=D_y)	6.2×10^{-6}	$D_a/D_{\perp ac}$	8.9
D_c (=D_z)	1.8×10^{-4}	D_a/D_c	0.30

[a] 4 ns simulations; configuration stored every 2 ps; the first 2 ns of the mean-square displacement was used for determining the diffusion coefficients.

Table 2. Carbon Dioxide Diffusion Coefficients ($cm^2\ s^{-1}$) for Different Temperatures in δ-Form s-PS

	diffusion coefficient ($cm^2\ s^{-1}$)[a]		diffusion coefficient ($cm^2\ s^{-1}$)[a]
	T = 60 °C		
D_a (=D_x)	5.6×10^{-7}	D	2.3×10^{-7}
$D_{\perp ac}$ (=D_y)	~0	D_a/D_c	4.4
D_c (=D_z)	1.3×10^{-7}		
	T = 70 °C		
D_a (=D_x)	1.1×10^{-6}	D	4.5×10^{-7}
$D_{\perp ac}$ (=D_y)	~0	D_a/D_c	5.5
D_c (=D_z)	2.1×10^{-7}		
	T = 80 °C		
D_a (=D_x)	1.8×10^{-6}	D	7.7×10^{-6}
$D_{\perp ac}$ (=D_y)	1.7×10^{-8}	$D_a/D_{\perp ac}$	107
D_c (=D_z)	2.1×10^{-5}	D_a/D_c	0.08

[a] 4 ns simulations; configuration stored every 2 ps; the first 2 ns of the mean-square displacement was used for determining the diffusion coefficients.

respectively. For helium, diffusion coefficients have been calculated at four different temperatures between room temperature and 80 °C. Simulations with carbon dioxide have been performed at the same temperatures. However, the diffusion is so slow at 25 °C (typically, the diffusion coefficient of CO_2 is 1 order of magnitude lower than that of helium) that no statistically meaningful diffusion coefficients can be reported for this temperature. So, in Table 2, only CO_2 diffusion coefficients at 60, 70, and 80 °C are presented.

Diagonal components of the diffusion tensor have also been calculated separately. For both penetrants, the diffusion is anisotropic. The analysis of the results of our simulations has shown that for all temperatures and for both penetrants the minimum diffusivity corresponds to the direction perpendicular to the *ac* plane (denoted as $\perp ac$ and corresponding to the *y* direction in our Cartesian system). Moreover, according to diffusion pathways described in the previous section, maximum diffusivity is expected to occur in the *a* and *c* directions

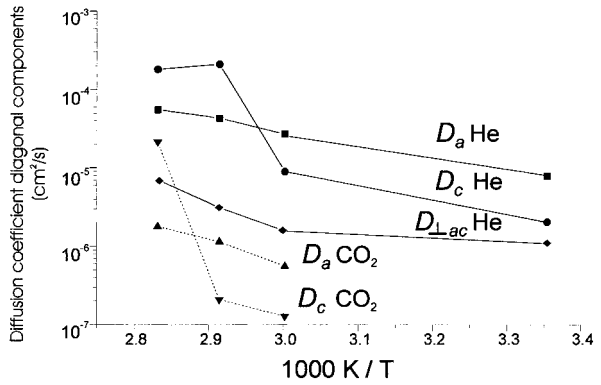

Figure 3. Anisotropy of penetrant diffusion in the δ crystalline form of s-PS. Diffusion coefficients for the motion along different crystallographic directions are shown for helium and CO_2: (■) helium motion along *a* (D_a); (●) helium motion along *c* (parallel to the chain axes; D_c); (◆) helium motion perpendicular to the *ac* plane ($D_{\perp ac}$); (▲) CO_2 motion along *a* (D_a); (▼) CO_2 motion parallel to the chain axes (D_c).

at low and high temperatures, respectively. Up to 60 °C, the diffusion of helium atoms along the *a* direction is much faster than that along the *c* (D_c) direction as well as that perpendicular to the *ac* plane ($D_{\perp ac}$). As expected, the diffusion coefficients rise with temperature (for He from $D = 3.7 \times 10^{-6}$ at 25 °C to 8.1×10^{-5} cm^2 s^{-1} at 80 °C). The individual components show a different temperature dependence: D_a and $D_{\perp ac}$ increase regularly with the temperature, while D_c presents an abrupt increase in the temperature range 60−70 °C. As a consequence, from 60 to 70 °C, the anisotropy ratio $D_a/D_{\perp ac}$ is poorly affected while the anisotropy ratio $D_c/D_{\perp ac}$ dramatically increases from 6 to 72 (correspondingly, the ratio D_a/D_c is reduced from 3.9 to 0.3). This suggests a preferred diffusion parallel to the helices at higher temperatures. The Arrhenius plot of D_c and D_a (Figure 3) indicates that, for helium, the crossover temperature for which $D_c = D_a$ is at roughly 65 °C.

A similar behavior is found for the diffusion of CO_2 molecules. At 60 °C, diffusion in the *a* direction ($D_a = 5.6 \times 10^{-7}$ cm^2 s^{-1}) is 5 times faster than that in the *c* (D_c) direction, with $D_{\perp ac}$ being so small at this temperature that it cannot be determined. For higher temperatures, diffusion coefficients become higher (from $D = 2.2 \times 10^{-7}$ cm^2 s^{-1} at 60 °C to 7.7×10^{-6} cm^2 s^{-1} at 80 °C). Also for CO_2, as the temperature increases, D_c rises faster than D_a and $D_{\perp ac}$. Correspondingly, the anisotropy ratio D_a/D_c decreases from 4.4 to 0.08, indicating a switch to a preferred CO_2 diffusion parallel to polymer chains, with the crossover between 70 and 80 °C (Figure 3). The change in the preferential diffusion from the *a* direction at low temperatures to parallel to the helix direction (*c* direction) is more pronounced for carbon dioxide than for helium, probably because of its larger size. Figure 3 indicates that the difference between the two molecules is mainly caused by a difference of the apparent activation energy for the diffusion in the *c* direction. The (admittedly not very well-defined) slope of D_a is quite similar for He and CO_2, whereas the absolute value of the slope of D_c is considerably larger for CO_2 than for He.

The large diffusional anisotropy and its abrupt temperature dependence cannot be explained by the standard diffusion mechanism for small penetrants in amorphous polymers. Although, as usual, hopping events are facilitated by transient channels of free volume between existing cavities and the channels are formed by thermal motions of the host polymer atoms,[1,2] for a nanoporous crystal phase average sizes and locations of the cavities, as well as crystallographic directions of the channels, are all identical.

As the temperature increases, *a* and *b* unit cell parameters increase (up to 1% from 25 to 80 °C) while the *c* unit cell parameter (corresponding to the chain periodicity) remains practically constant. This kind of anisotropy of the thermal expansion coefficients is usual in polymer crystals.[31] It is caused by the difference in stiffness of the atom−atom interactions in different directions. In the planes perpendicular to the chain axes, polymer chains experience soft van der Waals interactions, while along the *c* direction they have stiff bond-length and bond-angle potentials. At a given temperature this anisotropic dilation of the crystal phase allows the formation of transient channels along the [001] direction which become suitable for guest crossing. According to this picture, the crossover temperature, for CO_2, because of its larger size, is higher.

Conclusions

MD studies of the transport of the gaseous penetrants helium and carbon dioxide through crystalline s-PS in its nanoporous δ crystal form have been performed. They show, first, for both helium and CO_2 and for all considered temperatures a low diffusivity through the *ac* plane. As a consequence, a strong diffusional anisotropy at low and high temperatures has always been obtained. For low temperatures, preferential diffusion pathways, between neighbor cavities along ⟨101⟩ directions, lead to the maximum diffusivity being along the *a* direction. At higher temperatures, prevailing diffusion pathways and maximum diffusivity are in the *c* direction (parallel to the helices). The crossover temperature as well as the magnitude of the anisotropy change depends on the penetrant. This is explained by anisotropic unit cell deformation that facilitates transport in the *c* direction. The implications for much larger penetrants such as solvent molecules still have to be explored.

The findings of this paper can be compared to those of the (to our knowledge) only other MD study of small penetrant diffusion in a polymer crystal.[6] There, the diffusion of methane and carbon dioxide in crystalline isotactic PMP showed only a small, if any, diffusional anisotropy, which slightly favored motion parallel to the helices by $D_{||}/D_{\perp} = 1.1$ (methane) and 1.1−1.5 (carbon dioxide). This difference can be understood by the different packings and, in particular, by the presence of closely packed parallel helices in the ac plane for the δ form of s-PS (Figure 1A).

(31) No quantitative experimental information is available for temperature effects on the δ-form s-PS crystal lattice parameters; however, dilation of unit cell constants with temperature obtained in our simulation compares qualitatively well with experimental and simulation data for other polymeric crystals (see, e.g., refs 32−34).

(32) Dadobaev, G.; Slutsker, A. I. *Sov. Phys. Solid State* **1981**, *23*, 1131.

(33) Martoňák, R.; Paul, W.; Binder, K. *J. Chem. Phys.* **1997**, *106*, 8918

(34) Martoňák, R.; Paul, W.; Binder, K. *Phys. Rev. E* **1998**, *57*, 2425.

The fact that our simulations do show anisotropic diffusivity in δ-form s-PS crystals is very encouraging for the preparation of new membrane materials. The material is an easily processable *thermoplastic molecular sieve*, consisting of amorphous as well as δ-crystalline regions. The good definition of the cavity shapes has already been employed to achieve selectivity on sorption properties. In oriented semicrystalline samples, it would be possible to exploit the directional diffusivity of the material as well.

Recently developed experimental techniques seem to allow the preparation of s-PS films with different kinds of crystal orientations.[16] In particular, besides the axial orientation (orientation of the chain axes with respect to the main drawing direction), also a uniplanar orientation involving parallelism of the *ac* plane with respect to the film surface has been achieved.[16] Experimental studies on the permeability are in progress for both oriented and unoriented δ-form s-PS samples.

Acknowledgment. Financial support of the "Ministero dell'Istruzione, dell'Università e della Ricerca" (PRIN 2000 and CLUSTER 26) and of the National Research Council of Italy (CNR) for a Short Term Mobility grant for G.M. is greatly appreciated. We thank Oliver Biermann of MPI für Polymerforschung, Prof. Luigi Cavallo and Dr. Vincenzo Venditto of the University of Salerno, and Prof. Giuseppe Mensitieri of the University of Naples for useful discussions.

CM011297I